Effect of argon/hydrogen plasma cleaning on electroless ni deposition on small-area al pads

Ikeda, Akihiro
Graduate School of Information Science and Electrical Engineering, Kyushu University

Kajiwara, Kouhei
Graduate School of Information Science and Electrical Engineering, Kyushu University

Watanabe, Naoya
Graduate School of Information Science and Electrical Engineering, Kyushu University

Asano, Tanemasa
Graduate School of Information Science and Electrical Engineering, Kyushu University

出版情報：Japanese Journal of Applied Physics. 49 (8 PART 2), pp.08JA05(1)-08JA05(4), 2010-08.
The Japan Society of Applied Physics
バージョン：

Effect of Argon/Hydrogen Plasma Cleaning on Electroless Ni Deposition on Small-Area Al Pads

Akihiro Ikeda, Kouhei Kajiwara, Naoya Watanabe*, and Tanemasa Asano

Graduate School of Information Science and Electrical Engineering, Kyushu University, Fukuoka 819-0395, Japan

* On leave from Fukuoka Industry, Science and Technology Foundation (Fukuoka IST).

We investigated effect of Ar/H_2 plasma cleaning on electroless Ni under-bump metallurgy (UBM) layer formation on small-area Al pads. When 5×5 μm^2 pads are cleaned with the plasma, electroless Ni grows successfully on them, whereas no growth occurs on pads cleaned with conventional wet chemicals. In the Ni-UBM layer formation process, Zn is deposited by displacement plating on the Al pads before the electroless Ni plating. Microscopic observations, however, reveal that Zn is not successfully deposited on the wet-cleaned Al-pad surface. X-ray chemical analysis indicates that the plasma cleaning effectively removes C contaminations even for small pad sizes.

1. Introduction

In flip-chip assembly, solder bumps are used to connect a chip to the mounting board. An increase in chip functionality requires an increase in the number of input/output (I/O) pads, which in turn requires a reduction in the pad size and pitch.

In general, an under-bump metallurgy (UBM) layer is placed under the solder bumps. Electroless Ni is widely used as the UBM layer because it offers good adhesion to the solder and a slow reaction rate for the formation of the Ni_3Sn_4 intermetallic compound.[1,2] Deposition of electroless Ni on Al I/O pads requires a complex pretreatment. Because Al is not catalytically active for reducing agents such as hypophosphorous acid or dimethylamine borane in electroless Ni-plating solution, a Zn displacement plating on Al pads is required before electroless Ni plating.[3-5] Aluminum lacks an inner vacant electron orbit, which is generally needed for oxidation of a reducing agent at the Al surface (supplying electrons from the reducing agent to the Al) at the initial stage of Ni plating,[3] and Al is very subjective to oxidation. The Al surface-oxidation layer prevents chemical reaction with the reducing agent at the Al surface. However, a Zn displacement plating on the Al pads can eliminate these obstacles to electroless Ni plating.

Because Zn displacement platings are sensitive to surface contamination of Al, alkaline and acid wet cleaning has been used to remove organic contaminants from the Al pad surface.[4,5] However, with ever-decreasing I/O pad sizes, conventional wet cleaning will become insufficient to remove contaminations on Al pads. Another cleaning technique is plasma cleaning, which is widely used for cleaning bonding pads before wire bonding.[6-8] In the present study, we use Ar/H_2 plasma cleaning before Zn displacement plating on Al pads as small as $5 \times 5\ \mu m^2$. We use microscopic observation, chemical analysis, and fluid simulation to understand the effect of plasma cleaning on electroless Ni deposition.

2. Experimental Procedure

Electroless-Ni UBM layer formation was performed on chips diced from a test wafer and with Al pads. Figure 1 lists the Ni-UBM layer formation steps used in this study for either wet cleaning or plasma cleaning. The NaOH cleaning was performed to remove organic contaminants on the Al pads, then HNO_3 cleaning was performed to remove the residual smut generated by the NaOH cleaning. Next, the chip was dipped in the Zn displacement plating solution (Okuno Chemical Substar-AZ), which contained 2.9 wt% buffered hydrofluoric acid to remove native oxides on the Al pads. Because double Zn plating treatment is reported to improve the adhesion strength of Ni to the Al pads,[5] a second Zn plating was performed after

removal of the first Zn layer by the Zn etching solution (HNO_3). After the double-Zn plating, electroless Ni plating was performed. The electroless Ni plating solution (Okuno Chemical Top-Chemi-Alloy-B1) contained dimethylamine borane as a reducing agent of Ni ions. The boron concentration in the plated Ni was typically less than 1 wt%.

For Ni UBM layer formation with plasma cleaning, we exposed the chip to an Ar/H_2 plasma instead of dipping the chip in the wet cleaning solutions. A single-turn loop antenna was used to generate an inductively coupled plasma (ICP). The Ar/H_2 gas flow rate was 5/5 sccm; for cleaning, the gas pressure in the plasma chamber was 1 Pa; the exposure time was 1 min; the rf power for plasma generation was 1 kW; and the bias power for Ar-ion acceleration to the wafer was 50 W.

The Zn deposition processes were performed a few minutes after the wet cleaning or the plasma cleaning, and the scanning electron microscopy-energy dispersive analysis of X-rays (SEM-EDX) were performed a few hours after the wet or the plasma cleaning.

3. Results

3.1 Pad observations by focused ion beam-scanning ion microscopy

Figures 2(a) to 2(c) show images, acquired using a focused ion beam, scanning ion microscopy (FIB-SIM), of wet-cleaned Al pads after a first Zn plating, a second Zn plating, and a Ni plating, respectively. The pad size was 5×5 μm^2. The images were captured after cutting the pads at the center using the FIB, then tilting the sample by 45°. Figure 3(a) indicates that the first Zn plating deposited particle-like Zn on the pad, and a considerable area of the pad was not covered by Zn. After the second Zn plating, it appears that no Zn was deposited on the pad [see Fig. 2(b)]. Because of the failure of the Zn deposition, no Ni was deposited on the pad, as shown in Fig. 2 (c).

Figures 3(a) to 3(c) show FIB-SIM images of the plasma-cleaned pads after a first Zn plating, a second Zn plating, and a Ni plating, respectively. The pad size was 5×5 μm^2. In contrast to wet cleaning, for the plasma cleaning the Zn layer was deposited over the entire area of the pads for both the first and second Zn plating [see Figs. 3(a) and 3(b)]. In addition, the Ni was successfully deposited on the pad [see Fig. 3(c)].

Figures 4(a) and 4(b) show FIB-SIM images of the Al pads after Ni plating with wet cleaning and plasma cleaning, respectively. The pad size was 10×10 μm^2. We see that Ni grew on both the wet- and the plasma-cleaned pads. Thus, for large pad sizes, electroless plating can be performed even when the pads are wet cleaned. However, the Ni film deposited on wet-cleaned pads tends to become rough, whereas the surface of the Ni film on the plasma-

cleaned pad is smooth.

3.2 SEM-EDX analysis

From the FIB-SIM results presented above, we find that it is not possible to deposit sufficient Zn on wet-cleaned Al pads when the pad size is as small as 5 × 5 μm^2. To understand why there is insufficient Zn deposition with wet cleaning, we used SEM-EDX analysis to evaluate the atomic composition of the pads after wet cleaning or plasma cleaning. The area measured using SEM-EDX did not include the passivation surface layer (SiN) of the test chip, but was restricted to the pad surface.

Figures 5(a) and 5(b) show the EDX spectrum taken from the pads (5 × 5 μm^2 in size) after wet cleaning or plasma cleaning, respectively. The C Kα signal at 0.277 keV is stronger for the wet-cleaned pad than for the plasma-cleaned pad, which indicates that the efficiency of removal of the C contamination is poorer for the wet-cleaned pad than for the plasma-cleaned pad.

Figure 6 shows the C/Al atomic ratios deduced from the SEM-EDX spectrum. For the 5 × 5 μm^2 pads, more C is detected on the wet-cleaned pads than on the plasma-cleaned pads. However, the 10 × 10 μm^2 wet-cleaned pads exhibit a lower C contamination than the 5 × 5 μm^2 wet-cleaned pads.

We note that the test wafer used in this study was stored in a plastic wafer-storage box made of polycarbonate and polypropylene, and it has been reported that these storage boxes induce organic contamination of the wafer surface.[9,10)] In addition, the storage box that contained the wafers was stored in ambient air. Thus, the C contamination detected on the wet-cleaned pads might be caused by organic volatiles from the wafer-storage box and/or ambient air in the box.

4. Discussion

The SEM-EDX analysis suggests that the efficiency of C removal by wet cleaning degrades upon decreasing the pad size from 10 × 10 to 5 × 5 μm^2. To better understand this degradation in the efficiency of C removal, we performed a two-dimensional fluid simulation of the wet cleaning of the pad using ANSYS ED Ver. 5.6. In the simulation, the Al pad for Ni UBM layer formation was placed at the bottom of the via in the chip-passivation layer. The depth of the via was 0.85 μm as measured from the surface of the passivation layer. The sizes of the simulated pad were the same as that used in the experiment.

Figures 7(a) and 7(b) show the velocity vector distribution of water flowing over the pad

via with pad widths of 5 and 10 μm, respectively. The length of the arrow in Fig. 7 defines the magnitude of the velocity vector, and we assumed that the water flow was from left to right in the simulation area. The flow speed at the inlet boundary was defined as 1 cm/sec.

Figure 7 indicates that the water flow almost disappears at the corner of the pad via, and this phenomenon is observed for both the 5- and the 10-μm pads. Furthermore, we find that vortex flow is generated at the corner of the pad via. In the vortex flow region, cleaning by-products are trapped in the vortex and not removed from the pad via. The flow retardation effect at the corner is more significant for the 5-μm pad than for the 10-μm pad. Furthermore, except for the vortex region, the lateral flow speed above the 5-μm pad is slower than for the 10-μm pad. The averaged lateral flow speed near the surface of the 5-μm pad is 60% that of the 10-μm pad.

For the simulation, we assume that the water flow speed is 1 cm/s at the inlet boundary. During the experimental wet cleaning session, the cleaning solution was rotated manually by rotating the glass beaker containing the cleaning solution, so the actual flow speed of the cleaning solution may have been somewhat different from the simulated flow speed of 1 cm/s at the inlet boundary. To check the effect of the flow speed, we performed simulations with inlet flow speeds ranging from 0.1 to 10 cm/s. The results indicate that the flow is qualitatively the same as that for an inlet flow speed of 1 cm/s. Because the actual flow speed may be within the range of the simulated flow speeds (i.e., between 0.1 and 10 cm/s), the simulation results should represent the tendency of actual flow. Therefore, we conclude that the degradation in the C removal efficiency for the 5×5 μm^2 pad under these experimental conditions may be caused by an increased accumulation of cleaning by-product in the pad via because of the slower flow speed of the cleaning solution over the pad.

5. Conclusions

In anticipation of future large-scale integrated chips, we evaluate in this study the effect of Ar/H_2 plasma cleaning for electroless Ni UBM layer formation on small-area Al pads. We find that plasma cleaning effectively removes C contamination from the Al surface, even for pads as small as 5×5 μm^2. Thus, we conclude that Zn displacement plating and electroless Ni deposition can be performed using plasma cleaning.

We also perform a fluid simulation that suggests that the poor C removal efficiency of wet cleaning for small-area pads is caused by the accumulation of cleaning by-products in the pad via due to vortex flow at the pad-via corner and a reduction in the flow of the cleaning solution above the pad surface.

References

1) K. N. Tu and K. Zeng: Mater. Sci. Eng. R34 (2001) 1.

2) A. J. G. Strandjord, S. Popelar, and C. Jauernig: Microelectron. Reliab. 42 (2002) 265.

3) K. L. Lin and S.Y. Chang: Thin Solid Films 288 (1996) 36.

4) D. A. Hutt, C. Liu, P. P. Conway, D. C. Whalley, and S. H. Mannan: IEEE Trans. Components Packag. Technol. 25 (2002) 87.

5) M. K. M. Arshad, I. Ahmad, A. Jalar, G. Omar, and U. Hashim: J. Electron. Packag. 128 (2006) 246.

6) L. England and T. Jiang: Proc. Electronic Components and Technology Conf., 2007, p. 1604.

7) J. Park, H. J. Cha, B. S. Kim, Y. B. Jo, J. K. Park, S. Y. Kim, S. C. Shin, M. Y. Shin, K. I. Ouh, and H. Jeon: IEEE Trans. Components Packag. Technol. 30 (2007) 731.

8) Y. F. Chong, R. Gopalakrishnan, C. F. Tsang, G. Sarkar, S. Lim, and S. Tatti: Microelectron. Reliab. 40 (2000) 1199.

9) H. Habuka, Y. Shimazaki, S. Okamura, F. Sugimoto, T. Takeuchi, M. Aihara, M. Shimada, and K. Okuyama: Jpn. J. Appl. Phys. 42 (2003) 1575.

10) H. M. Park, Y. M. Kim, C. S. Cheong, J. C. Ryu, D. W. Lee, and K. B. Lee: Anal. Sci. 18 (2002) 477.

Figure captions

Fig. 1. Electroless-Ni UBM process using wet cleaning or plasma cleaning.

Fig. 2. 5 × 5 μm^2 Al pads cleaned with the wet chemical process after (a) first Zn plating, (b) second Zn plating, and (c) Ni plating.

Fig. 3. 5 × 5 μm^2 Al pads cleaned with the plasma process after (a) first Zn plating, (b) second Zn plating, and (c) Ni plating.

Fig. 4. 10 × 10 μm^2 Al pads after Ni plating with the (a) wet cleaning and (b) plasma cleaning.

Fig. 5. EDX spectrum of the 5 × 5 μm^2 Al pads after (a) wet cleaning and (b) plasma cleaning.

Fig. 6. Atomic ratio C/Al of the Al pads.

Fig. 7. Velocity vector distribution of water flow near the pad vias. The width of the pad via is (a) 5 and (b) 10 μm. The depth of the pad via is 0.85 μm for both (a) and (b).

Figures

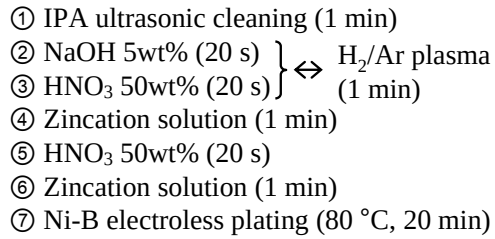

Fig. 1. Electroless-Ni UBM formation process using the wet cleaning or the plasma cleaning.

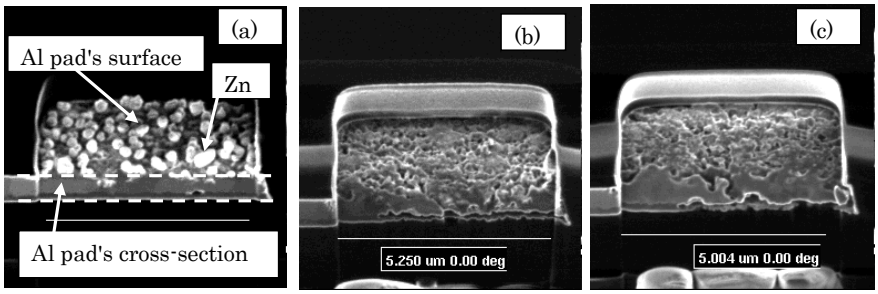

Fig. 2. 5 × 5 μm size Al pads cleaned with the wet chemical process after (a) 1st Zn plating, (b) 2nd Zn plating, (c) Ni plating.

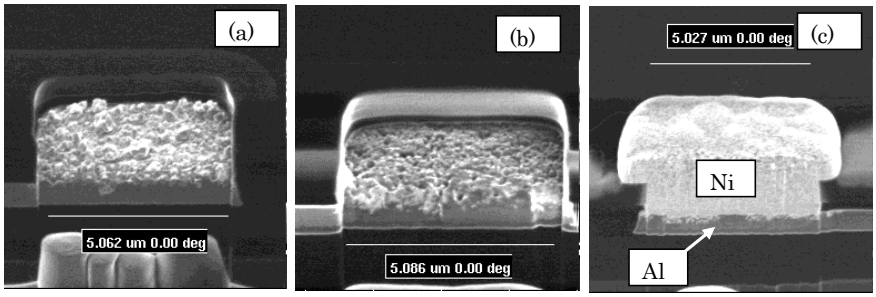

Fig. 3. 5 × 5 μm size Al pads cleaned with the plasma process after (a) 1st Zn plating, (b) 2nd Zn plating, (c) Ni plating.

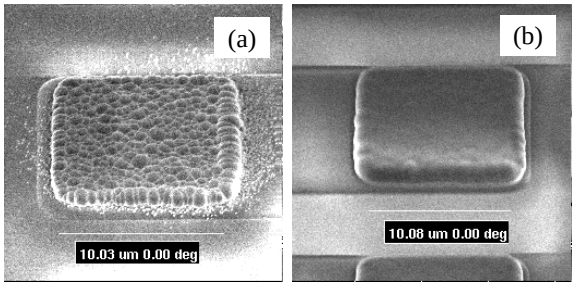

Fig. 4. 10 × 10 μm size Al pads after the Ni plating with the (a) wet cleaning, (b) plasma cleaning.

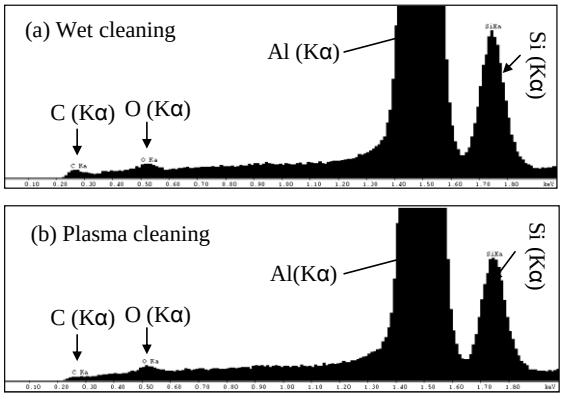

Fig. 5. EDX spectrum of the 5 × 5 μm size Al pads after the (a) wet cleaning, (b) plasma cleaning.

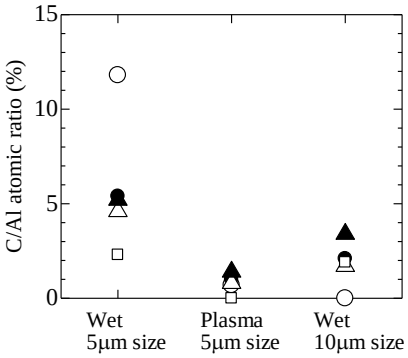

Fig. 6. C / Al atomic ratio of the Al pads.

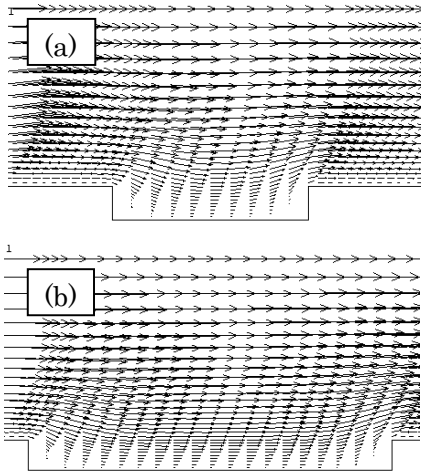

Fig. 7. Velocity vector distributions of water flowed near pad vias. The width of the pad via was (a) 5 μm, (b) 10μm. The depth of the pad via was 0.85 μm for both the (a) and (b).